

Technical University of Denmark



Fourier domain mode-locked swept source at 1050 nm based on a tapered amplifier

Marschall, Sebastian; Klein, Thomas; Wieser, Wolfgang; Biedermann, Benjamin R.; Hsu, Kevin; Hansen, Kim P.; Sumpf, Bernd; Hasler, Karl-Heinz; Erbert, Götz; Jensen, Ole Bjarlin; Pedersen, Christian; Huber, Robert; Andersen, Peter E.

Published in:
Optics Express

Link to article, DOI:
[10.1364/OE.18.015820](https://doi.org/10.1364/OE.18.015820)

Publication date:
2010

Document Version
Publisher's PDF, also known as Version of record

[Link back to DTU Orbit](#)

Citation (APA):
Marschall, S., Klein, T., Wieser, W., Biedermann, B. R., Hsu, K., Hansen, K. P., ... Andersen, P. E. (2010). Fourier domain mode-locked swept source at 1050 nm based on a tapered amplifier. *Optics Express*, 18(15), 15820-15831. DOI: 10.1364/OE.18.015820

DTU Library

Technical Information Center of Denmark

General rights

Copyright and moral rights for the publications made accessible in the public portal are retained by the authors and/or other copyright owners and it is a condition of accessing publications that users recognise and abide by the legal requirements associated with these rights.

- Users may download and print one copy of any publication from the public portal for the purpose of private study or research.
- You may not further distribute the material or use it for any profit-making activity or commercial gain
- You may freely distribute the URL identifying the publication in the public portal

If you believe that this document breaches copyright please contact us providing details, and we will remove access to the work immediately and investigate your claim.

Fourier domain mode-locked swept source at 1050 nm based on a tapered amplifier

Sebastian Marschall,^{1,*} Thomas Klein,² Wolfgang Wieser,² Benjamin R. Biedermann,² Kevin Hsu,³ Kim P. Hansen,⁴ Bernd Sumpf,⁵ Karl-Heinz Hasler,⁵ Götz Erbert,⁵ Ole B. Jensen,¹ Christian Pedersen,¹ Robert Huber,² and Peter E. Andersen¹

¹*DTU Fotonik, Department of Photonics Engineering, Technical University of Denmark, Frederiksborgvej 399, 4000 Roskilde, Denmark*

²*Lehrstuhl für BioMolekulare Optik, Ludwig-Maximilians-Universität München, Oettingenstraße 67, 80538 München, Germany*

³*Micron Optics, Inc., 1852 Century Place NE, Atlanta, GA30345 USA*

⁴*NKT Photonics A/S, Blokken 84, DK-3460 Birkerød, Denmark*

⁵*Optoelectronics Department, Ferdinand-Braun-Institut, Leibniz-Institut für Höchstfrequenztechnik, Gustav-Kirchhoff-Straße 4, 12489 Berlin, Germany*

*sema@fotonik.dtu.dk

Abstract: While swept source optical coherence tomography (OCT) in the 1050 nm range is promising for retinal imaging, there are certain challenges. Conventional semiconductor gain media have limited output power, and the performance of high-speed Fourier domain mode-locked (FDML) lasers suffers from chromatic dispersion in standard optical fiber. We developed a novel light source with a tapered amplifier as gain medium, and investigated the FDML performance comparing two fiber delay lines with different dispersion properties. We introduced an additional gain element into the resonator, and thereby achieved stable FDML operation, exploiting the full bandwidth of the tapered amplifier despite high dispersion. The light source operates at a repetition rate of 116 kHz with an effective average output power in excess of 30 mW. With a total sweep range of 70 nm, we achieved an axial resolution of 15 μm in air ($\sim 11 \mu\text{m}$ in tissue) in OCT measurements. As our work shows, tapered amplifiers are suitable gain media for swept sources at 1050 nm with increased output power, while high gain counteracts dispersion effects in an FDML laser.

©2010 Optical Society of America

OCIS codes: (140.3600) Lasers, tunable; (250.5980) Semiconductor optical amplifiers; (260.2030) Dispersion; (110.4500) Optical coherence tomography; (140.5960) Semiconductor lasers.

References and links

1. D. Huang, E. A. Swanson, C. P. Lin, J. S. Schuman, W. G. Stinson, W. Chang, M. R. Hee, T. Flotte, K. Gregory, C. A. Puliafito, and J. G. Fujimoto, "Optical coherence tomography," *Science* **254**(5035), 1178–1181 (1991).
2. A. F. Fercher, C. K. Hitzenberger, G. Kamp, and S. Y. El-Zaiat, "Measurement of intraocular distances by backscattering spectral interferometry," *Opt. Commun.* **117**(1-2), 43–48 (1995).
3. G. Häusler, and M. W. Lindner, "'coherence radar' and 'spectral radar' – new tools for dermatological diagnosis," *J. Biomed. Opt.* **3**(1), 21–31 (1998).
4. M. Choma, M. Sarunic, C. Yang, and J. Izatt, "Sensitivity advantage of swept source and Fourier domain optical coherence tomography," *Opt. Express* **11**(18), 2183–2189 (2003).
5. S. R. Chinn, E. A. Swanson, and J. G. Fujimoto, "Optical coherence tomography using a frequency-tunable optical source," *Opt. Lett.* **22**(5), 340–342 (1997).
6. B. Golubovic, B. E. Bouma, G. J. Tearney, and J. G. Fujimoto, "Optical frequency-domain reflectometry using rapid wavelength tuning of a Cr⁴⁺:forsterite laser," *Opt. Lett.* **22**(22), 1704–1706 (1997).
7. R. Leitgeb, C. K. Hitzenberger, and A. F. Fercher, "Performance of fourier domain vs. time domain optical coherence tomography," *Opt. Express* **11**(8), 889–894 (2003).
8. W. Wieser, B. R. Biedermann, T. Klein, C. M. Eigenwillig, and R. Huber, "Multi-Megahertz OCT: High quality 3D imaging at 20 million A-scans and 4.5 GVoxels per second," *Opt. Express* **18**(14), 14685–14704 (2010).

9. S. H. Yun, G. J. Tearney, J. F. de Boer, and B. E. Bouma, "Motion artifacts in optical coherence tomography with frequency-domain ranging," *Opt. Express* **12**(13), 2977–2998 (2004).
10. C. Chong, T. Suzuki, K. Totsuka, A. Morosawa, and T. Sakai, "Large coherence length swept source for axial length measurement of the eye," *Appl. Opt.* **48**(10), D144–D150 (2009).
11. S. H. Yun, C. Boudoux, G. J. Tearney, and B. E. Bouma, "High-speed wavelength-swept semiconductor laser with a polygon-scanner-based wavelength filter," *Opt. Lett.* **28**(20), 1981–1983 (2003).
12. R. Huber, M. Wojtkowski, K. Taira, J. G. Fujimoto, and K. Hsu, "Amplified, frequency swept lasers for frequency domain reflectometry and OCT imaging: Design and scaling principles," *Opt. Express* **13**(9), 3513–3528 (2005).
13. R. Huber, M. Wojtkowski, and J. G. Fujimoto, "Fourier Domain Mode Locking (FDML): A new laser operating regime and applications for optical coherence tomography," *Opt. Express* **14**(8), 3225–3237 (2006).
14. B. Považay, K. Bizheva, B. Hermann, A. Unterhuber, H. Sattmann, A. F. Fercher, W. Drexler, C. Schubert, P. K. Ahnelt, M. Mei, R. Holzwarth, W. J. Wadsworth, J. C. Knight, and P. S. Russell, "Enhanced visualization of choroidal vessels using ultrahigh resolution ophthalmic OCT at 1050 nm," *Opt. Express* **11**(17), 1980–1986 (2003).
15. Y. Wang, J. S. Nelson, Z. Chen, B. J. Reiser, R. S. Chuck, and R. S. Windeler, "Optimal wavelength for ultrahigh-resolution optical coherence tomography," *Opt. Express* **11**(12), 1411–1417 (2003).
16. R. Huber, D. C. Adler, and J. G. Fujimoto, "Buffered Fourier domain mode locking: Unidirectional swept laser sources for optical coherence tomography imaging at 370,000 lines/s," *Opt. Lett.* **31**(20), 2975–2977 (2006).
17. S. Makita, M. Yamanari, and Y. Yasuno, "High-speed and high-sensitive optical coherence angiography," *Proc. SPIE* **7372**, 73721M (2009).
18. M. K. K. Leung, A. Mariampillai, B. A. Standish, K. K. Lee, N. R. Munce, I. A. Vitkin, and V. X. D. Yang, "High-power wavelength-swept laser in Littman telescope-less polygon filter and dual-amplifier configuration for multichannel optical coherence tomography," *Opt. Lett.* **34**(18), 2814–2816 (2009).
19. R. Huber, D. C. Adler, V. J. Srinivasan, and J. G. Fujimoto, "Fourier domain mode locking at 1050 nm for ultrahigh-speed optical coherence tomography of the human retina at 236,000 axial scans per second," *Opt. Lett.* **32**(14), 2049–2051 (2007).
20. B. R. Biedermann, W. Wieser, C. M. Eigenwillig, T. Klein, and R. Huber, "Dispersion, coherence and noise of Fourier domain mode locked lasers," *Opt. Express* **17**(12), 9947–9961 (2009).
21. M. Chi, O. B. Jensen, J. Holm, C. Pedersen, P. E. Andersen, G. Erbert, B. Sumpf, and P. M. Petersen, "Tunable high-power narrow-linewidth semiconductor laser based on an external-cavity tapered amplifier," *Opt. Express* **13**(26), 10589–10596 (2005).
22. B. Adhimoalam, M. E. Klein, I. D. Lindsay, P. Groß, C. J. Lee, and K.-J. Boller, "Widely and rapidly tunable semiconductor master-oscillator fiber amplifier around 1080 nm," *IEEE Photon. Technol. Lett.* **18**(24), 2683–2685 (2006).
23. P. Gross, B. Adhimoalam, M. E. Klein, I. D. Lindsay, K. Hsu, and K. Boller, "9-Watt CW Swept-Wavelength Diode-Oscillator Yb-Fiber-Amplifier System," in *Conference on Lasers and Electro-Optics/Quantum Electronics and Laser Science Conference and Photonic Applications Systems Technologies*, Technical Digest (CD) (Optical Society of America, 2006), paper CFG5.
24. Y. Wang, W. Liu, J. Fu, and D. Chen, "Quasi-distributed fiber bragg grating sensor system based on a fourier domain mode locking fiber laser," *Laser Phys.* **19**(3), 450–454 (2009).
25. S. Marschall, L. Thrane, P. E. Andersen, C. Pedersen, and K. Hsu, "Frequency-swept laser light source at 1050 nm with higher bandwidth due to multiple semiconductor optical amplifiers in series," *Proc. SPIE* **7168**, 716824 (SPIE, 2009).
26. M. Y. Jeon, J. Zhang, and Z. Chen, "Characterization of Fourier domain mode-locked wavelength swept laser for optical coherence tomography imaging," *Opt. Express* **16**(6), 3727–3737 (2008).
27. C. Jirauschek, B. Biedermann, and R. Huber, "A theoretical description of Fourier domain mode locked lasers," *Opt. Express* **17**(26), 24013–24019 (2009).
28. M. Haverkamp, G. Kochem, and K. Boucke, "Single mode fiber coupled tapered laser module with frequency stabilized spectrum," *Proc. SPIE* **6876**, 68761D (2008).
29. W.-Y. Oh, S.-H. Yun, G. J. Tearney, and B. E. Bouma, "115 kHz tuning repetition rate ultrahigh-speed wavelength-swept semiconductor laser," *Opt. Lett.* **30**(23), 3159–3161 (2005).

1. Introduction

Optical coherence tomography (OCT) has become an important technique for biomedical imaging [1]. OCT can be divided into two domains, namely time domain-OCT and frequency domain-OCT. During recent years, frequency domain-OCT [2, 3] has developed rapidly, because it allows for significantly increased imaging speed and higher sensitivity [4]. In frequency domain-OCT, the light back-scattered from the sample interferes with light from a reference path, creating an interference pattern in the optical frequency domain. To retrieve the relevant information, one must sample the spectrum of the light exiting the interferometer, which can be done in one of the following two ways: In spectral domain-OCT, a spectrometer

is used in conjunction with a broadband light source. Alternatively, one can use a simple photo detector and a narrowband light source that sweeps its wavelength rapidly over a broad range [5, 6]. The latter technique, called swept source-OCT, is well suited for high speed imaging at wavelengths above 1000 nm, because it needs only readily available photo diodes for the detection. Spectral domain-OCT in this wavelength range requires usually InGaAs-based line cameras. These are expensive and have low pixel numbers, leading to a limited OCT ranging depth [7]. The simpler detection method of swept source-OCT allows also for dual balanced detection and comparably easy implementation of multi-spot imaging setups [8]. Furthermore, swept source-OCT is less prone to fringe washout effects caused by sample motion [9], and it can provide very high ranging depths [10].

One common implementation of a swept source is a laser based on a fiber ring resonator comprising a semiconductor optical amplifier (SOA) as gain medium and a tunable filter for wavelength selection [11, 12]. In contrast to a free-space resonator, a fiber-based setup enables implementing the Fourier domain mode-locking (FDML) technique in order to overcome the limitation in sweep velocity given by the build-up time of laser light in the cavity [13]. The concept of FDML is to synchronize the sweep rate of the tunable filter, f_{sw} , with the cavity round trip frequency, f_{rt} , in order to sustain uninterrupted lasing. To fulfill the frequency matching condition $f_{sw} = f_{rt} = c / (n \cdot l_{res})$, where c is the speed of light, l_{res} the length of the resonator, and n its effective index of refraction, f_{rt} must be in the range of sweep rates supported by the filter. Typically, one decreases f_{rt} to some tens or hundreds of kilohertz with a delay line of several kilometers length.

Light in the wavelength region around 1050 nm is well suited for retinal imaging. It allows for deeper penetration into the choroid than visible light and does not suffer from water absorption as severely as light with a wavelength above 1100 nm [14]. Furthermore, the dispersion in water, the main constituent of the vitreous, is minimal in the 1050 nm region, which is beneficial for maintaining a high depth resolution [15]. However, there are some challenges for the implementation of swept sources. SOAs for this wavelength are not as well-developed as those for the telecom bands (1300 nm or 1550 nm) and have significantly lower saturation power. Therefore, one often needs to post-amplify the output light of the swept source with a second SOA. Even though the sample power has to be limited for biological samples, e. g. to a few milliwatts for retinal imaging at 1050 nm, additional power can be required in order to compensate for losses in the imaging setup or for other purposes. For instance, buffering allows to “rectify” the sweep direction [16] or to achieve ultra-high A-scan rates [8] by splitting the laser output during one sweep into several “copies” and delaying them relative to each other, albeit at a power penalty of at least 6 dB. There are also OCT applications with multiple beams scanning the sample in parallel [17, 18]. Provided sufficient beam spacing, each beam can illuminate its target spot with the full allowed intensity. Another problem in the 1050 nm range is chromatic dispersion in standard single-mode fiber. In an FDML swept source, dispersion in the delay line limits the achievable tuning bandwidth, because frequency synchronization for all wavelengths simultaneously is impossible [19]. Under these conditions, extended photon cavity lifetime is only possible in a narrow wavelength band, while other spectral components exhibit reduced transmission through the tunable filter [20].

We propose a novel FDML light source configuration for the 1050 nm range that allows for high output power and broad bandwidth. We introduce a tapered amplifier as an alternative gain medium. This semiconductor gain element features a far higher saturation power than conventional SOAs due to its particular architecture. Previously, Chi *et al.* used a tapered amplifier in a high-power laser, tunable around 800 nm [21]. Adhimoalam and Groß *et al.* demonstrated wavelength-swept lasers at 1080 nm with sweep rates from 0.1 to 1 kHz based on a tapered amplifier in a free-space ring resonator [22, 23]. Here, we present the integration of a tapered amplifier into a fiber-based swept source and prove its feasibility for high-speed FDML operation.

Furthermore, we investigate the influence of dispersion by comparing the FDML performance with two different fibers as delay line: a standard single-mode fiber and a low-dispersion photonic crystal fiber (PCF). With the PCF, the effects of dispersion are significantly reduced, but its high insertion loss leads to lower overall performance in comparison to the standard fiber.

In both configurations, we achieve high FDML performance with an additional conventional SOA in the resonator. The extra gain provided by the SOA does not only compensate for intrinsic losses, it also helps to overcome the bandwidth-limiting effects of dispersion in the standard fiber. Thus, we can exploit the full tuning bandwidth of the tapered amplifier even in conjunction with the dispersive delay line. In contrast to other configurations with equal gain media in series [18, 24, 25], we use two different amplifiers with complementary characteristics. The conventional SOA provides a large small-signal gain, while the tapered amplifier features high saturation power. This combination allows for stable FDML operation with high output power and broad bandwidth at the same time.

This paper presents the developed light source setup (Sec. 2). It discusses the results of the characterization, along with observations made during the measurements, and shows OCT images acquired with the light source (Sec. 3). After summarizing the results (Sec. 4), it provides an outlook on the possibilities for further development (Sec. 5).

2. Setup

This section provides an overview over the light source setup (Sec. 2.1) and describes in detail the key components and their role within the system, namely the tapered amplifier (Sec. 2.2), the delay line (Sec. 2.3), and the auxiliary SOA (Sec. 2.4). The latter section also includes a discussion on the relation of dispersion and gain in FDML lasers.

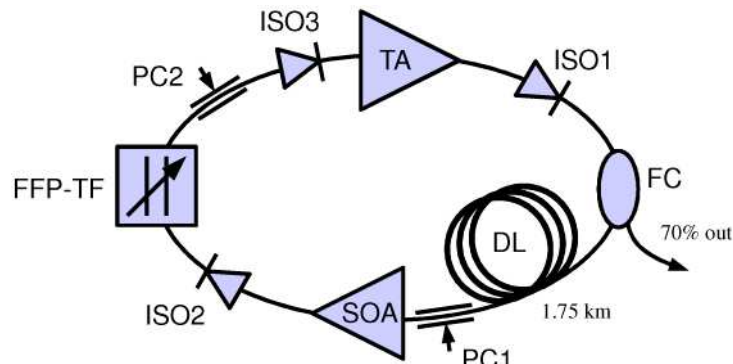


Fig. 1. Setup of the high-power FDML light source. TA: tapered amplifier including fiber-coupling optics; SOA: semiconductor optical amplifier, FFP-TF: fiber Fabry-Perot tunable filter; DL: delay line; FC: fiber coupler; ISO: optical isolator; PC: polarization controller.

2.1 Laser resonator

The developed light source setup (Fig. 1) is a fiber-based ring resonator. The key component is a tapered amplifier (Ferdinand-Braun-Institut, Leibniz-Institut für Höchstfrequenztechnik). Its output is focused into a single-mode fiber. A fiber coupler directs 70% of the light out of the cavity and the remaining 30% into a delay line (1.75 km fiber). An SOA (InPhenix) amplifies the light before it passes a fiber-coupled Fabry-Perot tunable filter (Micron Optics). The filter selects a narrow wavelength band (150 pm FWHM) that is fed back to the tapered amplifier. Optical isolators following the amplifiers and the filter ensure unidirectional lasing in the resonator and suppress back-reflections from the Fabry-Perot cavity. Polarization controllers in the cavity adjust the polarization state of the light at the amplifier inputs to match the axis of maximum gain. For practical reasons, we installed the polarization

controller for the tapered amplifier (PC2) on the input fiber of the isolator in front of it (ISO3).

2.2 Tapered amplifier

Tapered amplifiers are suitable gain media for fiber-based lasers with high output power. These devices are a type of SOA with a special waveguide architecture. On the input side, the waveguide has a straight narrow section that supports only the fundamental transverse mode of the light field. It is followed by the tapered section, where the waveguide slowly broadens, so that the mode field expands while maintaining its original single-mode profile. In contrast to conventional SOAs with a single-mode waveguide, tapered amplifiers allow for high drive currents (several amperes) and therefore provide high saturated output power (up to several watts), but still emit a beam of high quality, suitable for single-mode fiber coupling. We integrated a tapered amplifier into the fiber-resonator using free-space coupling optics (Fig. 2), because packaged and fiber-pigtailed modules are not yet commercially available.

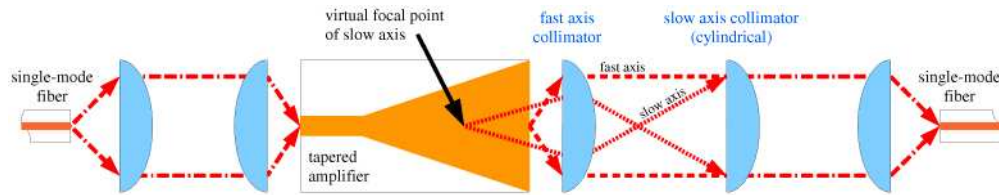


Fig. 2. The tapered amplifier is integrated into the fiber-based resonator by free-space coupling optics. Typical for tapered amplifiers is the astigmatism of the output beam. The fast axis (perpendicular to the taper plane, dashed arrows) emerges from a focal point on the crystal facet. The slow axis (within the taper plane, dotted arrows) has a virtual focal point within the tapered section. Therefore, an additional cylindrical lens is necessary to focus the light into a fiber.

The device we used is a single quantum well amplifier with a 1 mm long straight waveguide section and a 3 mm long tapered section with 4° full taper angle. With a drive current $I_{TA} = 2.5$ A at 25°C , the amplified spontaneous emission (ASE) band extends approximately from 1030 to 1080 nm (FWHM) with a peak at 1060 nm (Fig. 3).

In a preliminary experiment, we tested the tuning bandwidth of the tapered amplifier in a low-speed (non-FDML) swept source. The setup was a laser resonator similar to that described in Sec. 2.1, but without the delay line and the additional SOA. With $I_{TA} = 2$ A and a filter sweep rate $f_{sw} \leq 1$ kHz, we achieved a total sweep range from 1025 to 1085 nm, which corresponds well with the ASE bandwidth. For $f_{sw} > 1$ kHz, the backward scan output power decreased rapidly, and for $f_{sw} > 3$ kHz also the forward scan power drops. These sweep rates are relatively low compared to SOA-based swept sources, which can usually maintain several 10 kHz, because tapered amplifiers have a lower gain. Including the fiber-coupling, the small-signal gain of our amplifier is roughly 15 dB for $I_{TA} = 2.5$ A, while a typical fiber-coupled SOA features 20 dB or more. Concluding from these results, the tapered amplifier can most likely not provide sweep rates interesting for OCT imaging (≥ 10 kHz) when used in a non-FDML fiber-ring laser configuration.

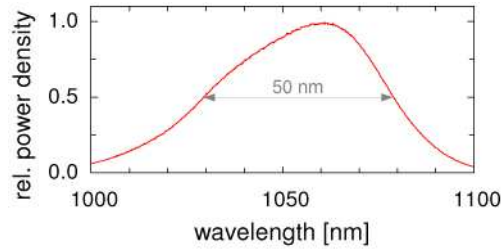


Fig. 3. Spontaneous emission spectrum of the tapered amplifier for 2.5 A drive current.

2.3 Delay line

The delay line decreases the resonator round trip frequency, allowing the sweep frequency of the tunable filter to be synchronized with it. The chosen length of 1.75 km results in a resonator round trip frequency of roughly 116 kHz, which is close to a mechanical resonance of the filter. We can thus achieve a large sweep amplitude with moderate drive currents.

We tested the light source using two different delay lines, one consisting of standard single-mode fiber and one made of a special low-dispersion photonic crystal fiber (PCF). The single-mode fiber (Corning HI-1060) has a low insertion loss, around 2 dB, but introduces a significant amount of chromatic dispersion. The longest and the shortest round trip time in the range of interest (1030 nm to 1100 nm) differ by approximately 4.5 ns. The PCF (NKT Photonics SC-5.0-1040) is tailored to have zero dispersion at 1040 nm. We do not have precise measurement data of the dispersion, but we estimated the maximum difference of round trip times to about 0.7 to 1.4 ns. The insertion loss of the PCF is comparably high for this application, around 10 dB. It originates partly from inherent attenuation (~3.8 dB/km according to the manufacturer test data) and partly from several splices between the PCF, the standard fiber that forms the rest of the resonator, and a mode-field adapting intermediate fiber.

2.4 Auxiliary SOA

The SOA is essential for high FDML performance. It increases the gain per round trip in the resonator substantially and compensates for the high insertion loss when the PCF delay line is used. In case of low loss and high dispersion, as with the HI-1060 delay line, the high gain counteracts the effects of dispersion, which would otherwise impair the FDML operation.

Several authors have studied how the dispersion-caused round trip mismatch affects an FDML light source. Huber *et al.* calculated a minimum line width for the tunable filter that allows light with a given mismatch to complete at least one round trip [19]. Biedermann *et al.* stated that the mismatch leads to reduced transmission through the tunable filter and estimated the maximum possible photon cavity lifetime in order to study the influence on the instantaneous laser line width [20].

Here, we investigate the effect of dispersion on the available FDML tuning bandwidth. Lasing is possible at wavelengths where the small-signal gain exceeds the total loss in the resonator. In addition to the intrinsic insertion loss of the components, dispersion leads under FDML operation to further wavelength-dependent loss in the tunable filter. This can be understood with the following consideration. Let the transmission window of the filter at time t_1 be centered at the wavelength λ_1 . The narrow band of transmitted light travels then once through the resonator within the round trip time $\tau_{rt}(\lambda_1)$. If the filter sweep period τ_{sw} matches $\tau_{rt}(\lambda_1)$, the light arrives at the filter when the transmission window is again centered at λ_1 , and passes with minimal loss. If the resonator exhibits chromatic dispersion, τ_{rt} does not equal τ_{sw} for most wavelengths. In this case, the transmission window and the band of arriving light are spectrally mismatched by $\lambda_{mis}(\lambda_1) = v_{sw}(\lambda_1) \cdot [\tau_{rt}(\lambda_1) - \tau_{sw}]$, where v_{sw} is the sweep velocity, i. e. the rate at which the filter wavelength changes (Fig. 4). The larger λ_{mis} is, the smaller is the

spectral overlap between the arriving light and the filter window, and hence the lower is the transmitted fraction of light. Towards the edges of the laser tuning spectrum where the small-signal gain is low, this additional loss can result in a negative net gain and thereby reduce the available tuning bandwidth.

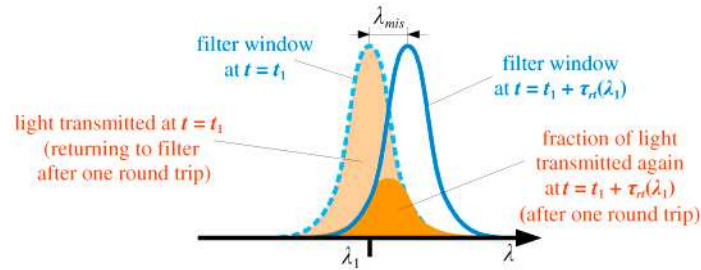


Fig. 4. Chromatic dispersion in an FDML resonator causes additional losses at the tunable filter. Light of wavelength λ_1 has passed the filter at time t_1 and returns after one round trip period $\tau_r(\lambda_1)$. If $\tau_r(\lambda_1)$ does not match the filter sweep period τ_{sw} , then the filter window is offset from λ_1 and only a reduced fraction of the light is transmitted again.

For known filter sweep characteristics and dispersion in the resonator, one could calculate the “dispersion loss” as a function of the wavelength and add this term to the net gain spectrum of the laser. However, this calculation would not take any effects into account that modify the spectrum of light travelling through the resonator. Especially, frequency down-conversion by non-linear effects in the semiconductor gain chips can increase or reduce the dispersion loss. In case of the bi-directionally sweeping Fabry-Perot filter, the transmission becomes thus asymmetric for the two sweep directions, as Jeon *et al.* described earlier [26]. A quantitative calculation must therefore at least include the gain dynamics of the involved amplifiers, as demonstrated by Jirauschek *et al.* [27]. However, this is beyond the scope of this work. Nevertheless, the considerations made above allow us to make a qualitative statement: dispersion in an FDML resonator causes additional loss which, to a certain extent, can be compensated by high gain.

While the tapered amplifier can generate very high output power, it has lower small-signal gain than a conventional SOA due to its lower confinement factor. For $I_{TA} = 2.5$ A, the fiber-coupled amplifier unit has a small-signal gain of about 15 dB (in contrast to about 20 dB of the SOA). Under non-ideal conditions, such as high dispersion or loss, the gain of the tapered amplifier alone is not sufficient for a well-operating FDML laser. In tests without the SOA, the light source showed only very poor FDML performance. The laser output fluctuated from sweep to sweep and exhibited strong relative intensity noise, while the total sweep bandwidth hardly exceeded 40 nm. Increasing the drive current up to 5 A did lead to slightly higher average power, but not to reduced fluctuations or noise. When we, on the other hand, tested the FDML laser with the SOA only, a sweep range up to 70 nm was possible, but with only few milliwatts of average power and with strong relative intensity noise.

In our novel configuration, the two different amplifiers work complementary: Like a pre-amplifier, the SOA raises the low light intensity at the end of the feedback loop to a useful input level for the tapered amplifier. The tapered amplifier then acts as a booster, providing high output power.

3. Results

This section covers the results of the light source characterization. First, we examine the operation characteristics of the system with both delay lines and discuss important observations (Sec. 3.1). Then, we compare the performance of both configurations in an interferometry setup and present images acquired with the light source (Sec. 3.2).

3.1 Light source characteristics

With the HI-1060 delay line, the light source allows for FDML operation with maximal tuning bandwidth for the sweep frequency f_{sw} ranging from 116.78 to 116.86 kHz. This is different from FDML systems at 1300 nm, where dispersion in the delay line is very low and the resonator round trip frequency f_{rt} is nearly constant within the entire sweep spectrum. At 1050 nm, f_{rt} varies significantly over the sweep range, so that the FDML operating frequency is no longer clearly defined.

The transient output power (Fig. 5a) shows a strong asymmetry between the forward sweep (from low to high wavelengths) and the backward sweep. If f_{sw} is tuned to the maximum round trip frequency within the sweep spectrum, $f_{rt,max}$, the light source runs stable with high output power during the forward sweep, while the backward sweep power decreases severely and is subject to strong amplitude fluctuations. For $f_{sw} = f_{rt,min}$ the performance degrades only during the forward sweep, and for $f_{rt,min} < f_{sw} < f_{rt,max}$ both sweep directions are partially affected.

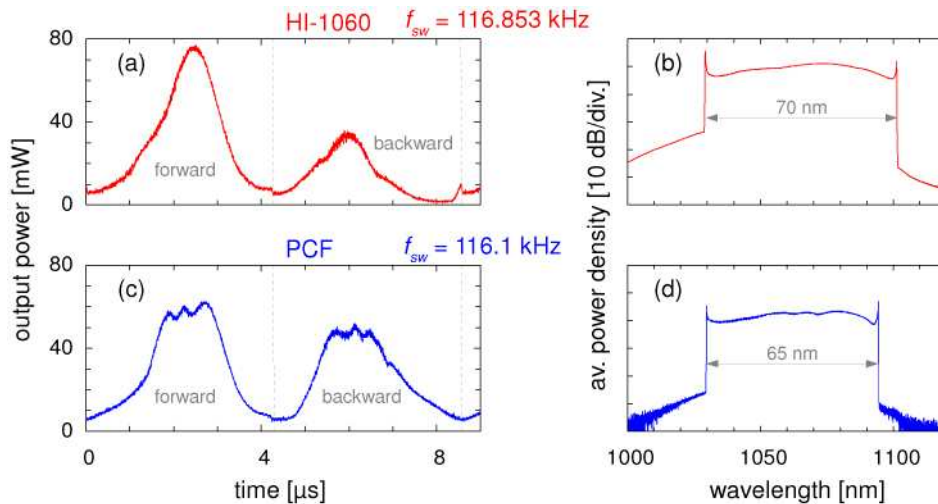


Fig. 5. The transient output power of the light source (a, c) is high, but there is a strong asymmetry between sweeping forward (increasing wavelength) or backward (decreasing wavelength). Even though the asymmetry is lower with the PCF-delay line, still only one sweep direction appears useful for OCT. As the averaged power spectra (b, d) show, the HI-1060 delay line allows for a slightly higher total sweep range than the PCF.

This phenomenon can be explained as a combined effect of chromatic dispersion in the delay line and frequency down-conversion due to non-linear processes in the semiconductor crystals. Because of the frequency shift, positive detuning of an FDML laser ($f_{sw} > f_{rt}$) affects the backward sweep significantly stronger than the forward sweep, and vice versa for negative detuning ($f_{sw} < f_{rt}$), as Jeon *et al.* discussed previously [26]. If $f_{sw} = f_{rt,max}$, the laser is positively detuned for the entire sweep range, and thus the performance deteriorates only during the backward sweep. Correspondingly, for $f_{sw} = f_{rt,min}$ only the forward sweep is severely affected. The effect is particularly strong in our light source setup, because there are two semiconductor gain chips in series that shift the frequency. As a result, only one sweep direction appears useful for high quality OCT imaging. In terms of power and stability, the light source performs best when it is tuned for optimal forward sweep operation.

The average output power for $f_{sw} = 116.853$ kHz and drive currents $I_{TA} = 2.3$ A and $I_{SOA} = 0.3$ A is 20 to 25 mW. During the forward sweep—which would be used for imaging—the average power is approximately 30 to 35 mW. These power levels are sufficient for most

ophthalmic applications. Even if one buffers the forward sweep in order to double the OCT A-scan rate, one has two outputs with at least 7 mW each to work with.

However, these output power levels are actually lower than expected. In a simple free-space cw-resonator, our tapered amplifier emitted several hundred milliwatts with 1 to 2 A drive current, and in general such devices can generate several watts of laser light [21, 28]. Apparently, the feedback in the current fiber-optic configuration is not sufficient to saturate the gain of the tapered amplifier. The SOA, on the other hand, works in the saturation regime and limits thereby the feedback to the tapered amplifier. In conjunction with losses caused by the fiber-coupling optics and the other components, this leads to the comparably low output. One could increase the power by optimizing the fiber-coupling, by using an SOA with higher saturation power, or by driving the tapered amplifier with a higher current.

The total sweep range is 70 nm (Fig. 5b), and the 3 dB-bandwidth after linearization in the optical frequency domain is 11.5 THz (~42 nm). This corresponds well with the tuning range of the tapered amplifier during the preliminary test (Sec. 2.2). Obviously, this FDML laser configuration exploits the gain bandwidth of the tapered amplifier very well, even though the resonator is subject to high chromatic dispersion. An adequate modulation of I_{SOA} during the sweep cycle can possibly increase the bandwidth even further by shaping the output spectrum flatter and broader.

With the PCF delay line, the sweep frequency range for FDML operation is narrower, 116.085 to 116.1 kHz, and the asymmetry in the transient output power (Fig. 5c) is significantly lower, both due to lower dispersion. Still, one sweep direction is subject to strong power fluctuations and does not appear useful for OCT. It is also difficult to adjust the polarization in order to achieve a smooth spectrum without dips. For $f_{sw} = 116.1$ kHz and the same drive currents as above, the forward sweep is stable and has an average power around 30 mW. The total sweep range is 65 nm (Fig. 5d) and the 3 dB-bandwidth roughly 42 nm.

The characteristics of both configurations are remarkably similar because of common limiting factors. The saturation power of the SOA limits the output power of the light source, whereas the gain bandwidth of the tapered amplifier limits the sweep bandwidth. Regarding the effects of dispersion, the PCF-configuration is clearly closer to the ideal case, where both sweep directions exhibit symmetric output power. But due to the very high insertion loss, it does not improve the overall performance in this light source embodiment. However, the PCF could be of advantage in a light source with higher gain bandwidth, where dispersion has a stronger impact, or with higher sweep frequency, where the delay line is shorter and hence the insertion loss is lower.

3.2 Interferometry and imaging

In order to test the performance of the light source for OCT imaging, we generated point spread functions (PSF) in a Mach-Zehnder interferometer (MZI) with variable path length difference, using the output during the forward sweep (Fig. 6). For both delay lines, the PSFs have a width (3 dB) of 15 μm , which is somewhat higher than the theoretical ideal value of 12 μm , assuming a Gaussian spectrum with 42 nm FWHM. Still, the resulting axial resolution of 11 μm in biologic tissue is adequate for OCT imaging.

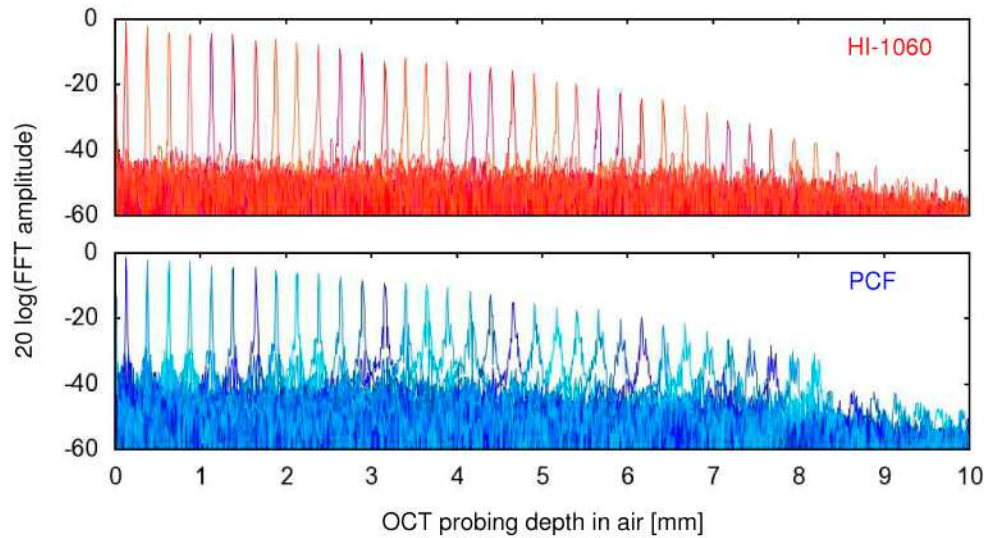


Fig. 6. The plots of point spread functions over a long range of OCT probing depths reveal better overall performance with the HI-1060 delay line (top). With the PCF (bottom), the signal roll-off is slightly slower, but the noise floor is higher and the point spread functions show larger side lobes, especially for long probing depths.

The signal roll-off as a function of the OCT probing depth z (optical path length difference divided by 2) is also similar for both fibers. An exponential fit to the PSF peaks (for $z \leq 6$ mm) shows 3.4 dB/mm roll-off for the HI-1060 delay line (6 dB at $z \approx 1.8$ mm) and 3.1 dB/mm for the PCF (6 dB at $z \approx 1.9$ mm). Besides the slightly better roll-off, the PSFs have larger side lobes—especially for long probing depths—and a higher noise floor in the PCF configuration.

Due to the better overall performance, we continued the work with the light source using the HI-1060 delay line. We measured a shot noise limited sensitivity of 110 dB for 10 mW sample arm power in the MZI with interferometer coupling losses taken into account.

In order to prove the OCT capability of the light source, we recorded images of a slice of cucumber and of human skin *in vivo*. The images consist of 1200 A-scans with 500 data points. Each A-scan was acquired within 2.5 μ s during the forward sweep of the light source with approximately 2.5 mW on the sample. The signal from the dual balanced detector was digitized at a rate of 400 MS/s with 12 bit resolution and 200 MHz analog bandwidth.

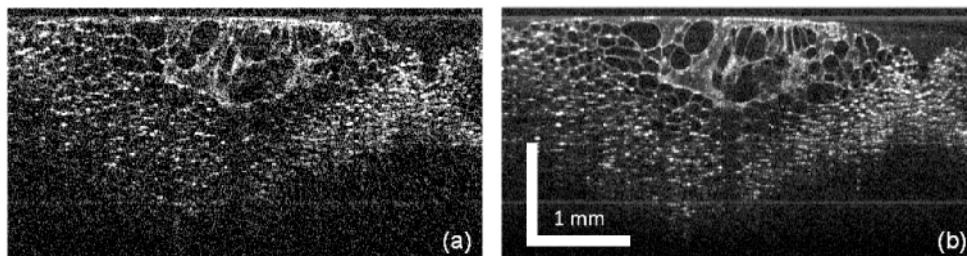


Fig. 7. OCT images of a slice of cucumber with a clearly visible cell structure and a penetration deeper than 1.5 mm into the water-rich tissue. The high imaging speed can be used to achieve a clearly visible reduction of the background noise, as the comparison of a single frame (a) and a sliding average over 10 frames (b) illustrates.

The cucumber images (Fig. 7) show clearly the cellular structure, and a penetration depth of more than 1.5 mm into the water-rich tissue is possible. Averaging over a number of B-frames can significantly reduce the noise, as the qualitative comparison of a single frame (Fig.

7a) and a sliding average over 10 B-scans (Fig. 7b) reveals. This shows the potential of speckle and background noise reduction while imaging at high speed. For the scale bar we assumed a refractive index of 1.33 in axial direction. The skin images were recorded at the finger tip (Fig. 8a) and the nail fold (Fig. 8b). A sliding average over 3 frames resulted in a good reduction of background noise. We rescaled the images assuming a refractive index of 1.4. Clearly visible features are the border between the thick stratum corneum at the finger tip and the lower parts of the epidermis, as well as the cross-section through the nail-plate and the epidermis structure in the cuticle region.

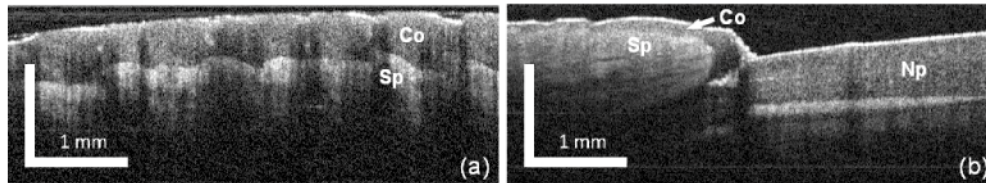


Fig. 8. OCT images of human skin in vivo. (a) Skin at the finger tip with a thick stratum corneum (Co) and a clearly visible border to the stratum spinosum (Sp). (b) Nail fold with a cross-section through the nail-plate (Np) and the epidermis structure in the cuticle region. The images are averaged over 3 frames.

4. Conclusion

We constructed an FDML swept source with a tapered amplifier as gain medium, sweeping bi-directionally at a repetition rate of 116 kHz with an average output power of more than 30 mW during the forward sweep. With a total sweep bandwidth of 70 nm, we achieved an axial resolution of 15 μm in air (11 μm in tissue). As the measured values for sensitivity (110 dB) and signal roll-off (3.4 dB/mm) indicate, the light source is suitable for OCT imaging, which we confirmed by acquiring a number of images.

We compared the light source performance using a standard single-mode fiber and a low-dispersion photonic crystal fiber as delay line. Although the effects of dispersion were clearly reduced with the PCF delay line, it did not improve the performance because of its high insertion loss. With the high gain of an auxiliary SOA, on the other hand, we exploited the full gain bandwidth of the tapered amplifier even with the dispersive standard fiber delay line.

These results bring two important insights for future swept source development. (1) Tapered amplifiers are suitable gain media, when high output power is required. (2) High gain counteracts the effects of dispersion in an FDML system and can help to maintain a high sweep bandwidth.

5. Future light source development

There are a number of possibilities both to improve our current swept source further and to continue research based on our results.

Due to the strong asymmetry of the output power between the two sweep directions, we used so far only the forward sweep for imaging. In other words, we operated with a 50% duty cycle. However, it would be straight forward to discard the backward sweep and to buffer the output in order to increase the A-scan to 233 kHz. Both outputs of the buffering stage would have sufficient power for OCT imaging (>7mW) without post-amplification.

One could also achieve a 100% duty cycle with full output power by using a tunable filter sweeping uni-directionally from low to high wavelengths. However, the fastest reported uni-directional sweep rate without buffering is 115 kHz [29]. In our case, we could therefore not increase the A-scan rate, only the exposure time. This could improve the imaging sensitivity, but at the same time, fringe wash-out effects due to sample motion might become stronger.

Even though the current configuration exploits the gain spectrum of the tapered amplifier very well, the sweep range can likely be broadened further by an adequate modulation of the

SOA drive current. The tapered amplifier we used is among those with the broadest gain bandwidth currently available. However, tapered amplifiers with even broader bandwidth are likely to be developed, and better OCT depth resolution may thus become possible.

By improving the feedback to the tapered amplifier, one can achieve higher output power, and one may expect reduced intensity noise and higher sensitivity. One could, for example, use an SOA with higher saturation power or optimize the fiber-coupling. The integration of a tapered amplifier into a fiber-pigtailed package, as demonstrated by Haverkamp *et al.* [28], could make the setup very stable and compact. As confirmed by preliminary tests, higher output power is also possible by increasing the tapered amplifier drive current. However, the fiber-coupling efficiency for higher currents must be investigated, and care has to be taken that none of the components in the resonator takes damage.

Although the low-dispersion fiber did not lead to superior performance in this light source embodiment, it still remains of interest for future swept source development. It might become useful for FDML lasers with higher sweep range, which are more severely affected by dispersion. Further studies are necessary to determine how large an amount of dispersion can be tolerated with sufficient gain, before actual dispersion-compensation becomes necessary. It is also possible to use the PCF in a light source with higher sweep frequency, since a shorter delay line has lower insertion loss.

Acknowledgments

S. Marschall, P. Andersen, R. Huber, T. Klein, W. Wieser, and B. Biedermann acknowledge financial support by the European Union project FUN OCT (FP7 HEALTH, contract no. 201880). Furthermore, R. Huber, T. Klein, W. Wieser, and B. Biedermann acknowledge funding by the Emmy Noether program of the German Research Foundation (DFG, HU 1006/2-1). K. Hsu acknowledges the funding award IIP-0724231 of the US National Science Foundation.